MSSM extensions (NMSSM) and Status of and ideas for Higgs sector searches

Jack Gunion
U.C. Davis

KITP2016 Experimental Challenges, April 26, 2016

Mostly a review of two papers: 1512.04281v2, Ellwanger and Rodríguez-Vázquez, who have updated Higgs issues in the NMSSM; and 1409.8393, Nils-Erik Bomark, Stefano Moretti, Shoaib Munir, Leszek Roszkowski who focused on light pseudoscalar situations.

NMSSM Basics

- The NMSSM differs from the MSSM due to the presence of the gauge singlet superfield S.

  In the simplest $\mathbb{Z}_3$ invariant realization of the NMSSM, the Higgs mass term $\mu H_u H_d$ in the superpotential $W_{\rm MSSM}$ of the MSSM is replaced by the coupling λ of S to H_u and H_d and a self-coupling κS^3.

  $W_{\rm NMSSM}$ is scale invariant and given by

$$W_{\rm NMSSM} = \lambda \hat{S} \hat{H}_u \cdot \hat{H}_d + \frac{\kappa}{3} \hat{S}^3 + \dots \ , \tag{1}$$

  where hatted letters denote superfields, and the ellipses denote the MSSM-like Yukawa couplings of $\hat{H}_u$ and $\hat{H}_d$ to the quark and lepton superfields.

  Once the real scalar component of $\hat{S}$ develops a vev s, the first term in $W_{\rm NMSSM}$ generates an effective μ-term

$$\mu_{\rm eff} = \lambda \, s \ . \tag{2}$$

- The soft Susy breaking terms consist of mass terms for the Higgs bosons H_u, H_d, S, squarks $\tilde{q}_i \equiv (\tilde{u}_{iL}, \tilde{d}_{iL})$, $\tilde{u}_{iR}^c$, $\tilde{d}_{iR}^c$ and sleptons $\tilde{\ell}_i \equiv (\tilde{\nu}_{iL}, \tilde{e}_{iL})$ and $\tilde{e}_{iR}^c$ (where $i = 1, 2, 3$ is a generation index):

$$\begin{aligned} -\mathcal{L}_0 &= m_{H_u}^2 |H_u|^2 + m_{H_d}^2 |H_d|^2 + m_S^2 |S|^2 + m_{\tilde{q}_i}^2 |\tilde{q}_i|^2 + m_{\tilde{u}_i}^2 |\tilde{u}_{iR}^c|^2 + m_{\tilde{d}_i}^2 |\tilde{d}_{iR}^c|^2 \\ &\quad + m_{\tilde{\ell}_i}^2 |\tilde{\ell}_i|^2 + m_{\tilde{e}_i}^2 |\tilde{e}_{iR}^c|^2 \,, \end{aligned} \tag{3}$$

trilinear interactions involving the third generation squarks, sleptons and the Higgs fields (neglecting the Yukawa couplings of the two first generations):

$$\begin{aligned} -\mathcal{L}_3 &= \Big(h_t A_t \, Q \cdot H_u \, \tilde{u}_{3R}^c + h_b A_b \, H_d \cdot Q \, \tilde{d}_{3R}^c + h_\tau A_\tau \, H_d \cdot L \, \tilde{e}_{3R}^c \\ &\quad + \lambda A_\lambda \, H_u \cdot H_d \, S + \frac{1}{3} \kappa A_\kappa \, S^3 \Big) + \text{h.c.} \,, \end{aligned} \tag{4}$$

and mass terms for the gauginos $\tilde{B}$ (bino), $\tilde{W}^a$ (winos) and $\tilde{G}^a$ (gluinos):

$$-\mathcal{L}_{1/2} = \frac{1}{2} \left[M_1 \tilde{B} \tilde{B} + M_2 \sum_{a=1}^{3} \tilde{W}^a \tilde{W}_a + M_3 \sum_{a=1}^{8} \tilde{G}^a \tilde{G}_a \right] + \text{h.c.} \,. \tag{5}$$

- In the CNMSSM one assumes that the soft Susy breaking terms involving gauginos, squarks or sleptons are identical at the GUT scale:

$$M_1 = M_2 = M_3 \equiv M_{1/2} \ , \tag{6}$$

$$m^2_{\tilde{q}_i} = m^2_{\tilde{u}_i} = m^2_{\tilde{d}_i} = m^2_{\tilde{\ell}_i} = m^2_{\tilde{e}_i} \equiv m_0^2 \ , \tag{7}$$

$$A_t = A_b = A_\tau \equiv A_0 \ . \tag{8}$$

- In the NUH-NMSSM, the Higgs soft mass terms $m^2_{H_u}$, $m^2_{H_d}$ and m^2_S are allowed to differ from m_0^2 (and determined implicitly at the weak scale by the three minimization equations of the effective potential), and the trilinear couplings A_λ, A_κ can differ from A_0. Hence the complete parameter space is characterized by

$$\lambda \ , \ \kappa \ , \ \tan\beta \ , \ \mu_{\rm eff} \ , \ A_\lambda \ , \ A_\kappa \ , \ A_0 \ , \ M_{1/2} \ , \ m_0 \ , \tag{9}$$

  where the latter five parameters are taken at the GUT scale.

  This NUH-NMSSM relaxation is more or less required to get $m_h \sim 125$ GeV, keeping CNMSSM for remaining parameters.

The NMSSM Higgs Sector

- Basics:

$$H_u = \begin{pmatrix} H_u^+ \\ H_u^0 = v_u + \frac{1}{\sqrt{2}}(H_{u,r}^0 + iH_{u,i}^0) \end{pmatrix}, \qquad H_d = \begin{pmatrix} H_d^0 = v_d + \frac{1}{\sqrt{2}}(H_{d,r}^0 + iH_{d,i}^0) \\ H_d^- \end{pmatrix}$$

$$S = s + \frac{1}{\sqrt{2}}(S_r + iS_i) \ . \tag{10}$$

Once the soft Higgs masses are expressed in terms of M_Z, $\tan\beta$ and s using the minimization equations of the potential, the Higgs sector of the NMSSM at tree level is described by six parameters

$$\lambda, \quad \kappa, \quad \tan\beta, \quad \mu = \lambda s, \quad A_\lambda \quad \text{and} \quad \mathrm{A}_\kappa \ . \tag{11}$$

- Defining $v^2 = 2M_Z^2/(g_1^2 + g_2^2) \sim (174\ \mathrm{GeV})^2$, the 3×3 CP-even mass matrix in the basis $(H_{d,r}, H_{u,r}, S_r)$ reads:

$$
\begin{aligned}
\mathcal{M}^2_{S,11} &= M_Z^2 \cos^2\beta + \mu(A_\lambda + \kappa s)\tan\beta \ , \\
\mathcal{M}^2_{S,12} &= (\lambda v^2 - \frac{M_Z^2}{2})\sin 2\beta - \mu(A_\lambda + \kappa s) \ , \\
\mathcal{M}^2_{S,13} &= \lambda v\left(2\mu\cos\beta - (A_\lambda + 2\kappa s)\sin\beta\right) \ , \\
\mathcal{M}^2_{S,22} &= M_Z^2 \sin^2\beta + \mu(A_\lambda + \kappa s)\cot\beta + \Delta_{\rm rad} \ , \\
\mathcal{M}^2_{S,23} &= \lambda v\left(2\mu\sin\beta - (A_\lambda + 2\kappa s)\cos\beta\right) \ , \\
\mathcal{M}^2_{S,33} &= \lambda A_\lambda \frac{v^2}{2s}\sin 2\beta + \kappa s(A_\kappa + 4\kappa s) \ . \qquad (12)
\end{aligned}
$$

Here $\Delta_{\rm rad}$ denotes the dominant radiative corrections due to top/stop loops,

$$
\Delta_{\rm rad} = \frac{3m_t^4}{4\pi^2 v^2}\left(\ln\left(\frac{m_T^2}{m_t^2}\right) + \frac{X_t^2}{m_T^2}\left(1 - \frac{X_t^2}{12 m_T^2}\right)\right) \qquad (13)
$$

where m_T is the geometrical average of the soft SUSY breaking stop masses, and $X_t = A_t - \mu/\tan\beta$ with A_t the soft SUSY breaking stop trilinear coupling.

- It is convenient to rotate $\mathcal{M}_S^2$ by an angle β in the doublet sector sector into $\mathcal{M}_S'^2$ in the basis H'_{SM}, H', S' (with $S' \equiv S_r$):

$$\mathcal{M}_S'^2 = R(\beta)\mathcal{M}_S^2 R^{\mathcal{T}}(\beta)\ , \qquad R(\beta) = \begin{pmatrix} \cos\beta & \sin\beta & 0 \\ \sin\beta & -\cos\beta & 0 \\ 0 & 0 & 1 \end{pmatrix}\ . \tag{14}$$

- Such a basis (also known as Higgs basis) has many advantages

1. Only the component H'_{SM} of the Higgs doublets acquires a vev v and, for realistic parameters, it is nearly unmixed.

   H'_{SM} has SM-like couplings to fermions and electroweak gauge bosons.
2. The possibly heavy doublet field H' is the CP-even partner of the MSSM-like CP-odd state A, but can mix.
3. S' remains (by definition) a pure singlet, but will mix.

- The mass matrix $\mathcal{M}'^2_S$ in the basis (H'_{SM}, H', S') has the elements

$$\begin{aligned}
\mathcal{M}'^2_{S,11} &= M_Z^2 \cos^2 2\beta + \lambda^2 v^2 \sin^2 2\beta + \sin^2\beta \Delta_{\rm rad} \ , \\
\mathcal{M}'^2_{S,12} &= \sin 2\beta \left(\cos 2\beta \left(M_Z^2 - \lambda^2 v^2 \right) - \frac{1}{2} \Delta_{\rm rad} \right) \ , \\
\mathcal{M}'^2_{S,13} &= \lambda v \left(2\mu - (A_\lambda + 2\nu) \sin 2\beta \right) \ , \\
\mathcal{M}'^2_{S,22} &= M_A^2 + \left(M_Z^2 - \lambda^2 v^2 \right) \sin^2 2\beta + \cos^2\beta \Delta_{\rm rad} \ , \\
\mathcal{M}'^2_{S,23} &= \lambda v (A_\lambda + 2\nu) \cos 2\beta \ , \\
\mathcal{M}'^2_{S,33} &= \lambda A_\lambda \frac{v^2}{2s} \sin 2\beta + \nu \left(A_\kappa + 4\nu \right) \ , \qquad (15)
\end{aligned}$$

where we have defined $\nu = \kappa s$ and

$$M_A^2 = \frac{2\mu}{\sin 2\beta} (A_\lambda + \nu) \ , \qquad (16)$$

the mass squared of the MSSM-like CP-odd state A. (A mixes, in principle, with a mostly singlet-like state A_S.)

- After an additional final diagonalization the eigenstates will be denoted as
  - H_{SM} (dominantly SM-like)
  - H_S (dominantly singlet-like) and
  - H (dominantly the MSSM-like heavy scalar).

- By this final diagonalization the state H_S picks up couplings to electroweak gauge bosons (vector bosons) proportional to the $H'_{SM} - S'$ mixing angle. Defining by κ_V the ratio of couplings of a Higgs state to vector bosons relative to the corresponding coupling of the SM-like Higgs boson, one has

$$\kappa_V^2(H_{SM}) + \kappa_V^2(H_S) + \kappa_V^2(H) = 1 \; . \tag{17}$$

  $H'_{SM}-S'$ mixing will necessarily generate $\kappa_V^2(H_S) \neq 0$ and hence reduce $\kappa_V^2(H_{SM})$, which is already and will be even more constrained by Higgs coupling measurements at the LHC.

- Similarly, the state H_S picks up couplings to fermions by both $H'_{SM} - S'$ and $H' - S'$ mixing, leading to non-vanishing values for $\kappa_U(H_S)$ (the reduced coupling of H_S to up-type quarks) and $\kappa_D(H_S)$ (the reduced coupling of H_S to down-type quarks). Then loop diagrams generate non-vanishing values for $\kappa_{gg}(H_S)$ (the

reduced coupling of H_S to gluons) and $\kappa_{\gamma\gamma}(H_S)$ (the reduced coupling of H_S to diphotons).

- It is important to note that the coupling of H_S to down-type quarks can suffer from cancellations among the contributions from $H'_{SM} - S'$ and $H' - S'$ mixing, respectively. This can result in a reduced branching fraction $BR(H_S \to b\bar{b})$.

  Since this decay constitutes the dominant contribution to the total width of H_S, its reduction implies enhanced branching fractions into other final states like $\gamma\gamma$.

  Hence, the $BR(H_S \to \gamma\gamma)$ can be larger than the one of a SM-Higgs boson of corresponding mass, leading to $\kappa_{\gamma\gamma}(H_S) > 1$.

- The diagonal term in (15) associated with the mass of the mostly SM Higgs is

$$\mathcal{M}'^2_{S,11} = M_Z^2 \cos^2 2\beta + \lambda^2 v^2 \sin^2 2\beta + \sin^2\beta \Delta_{\rm rad} \tag{18}$$

  where the first term is the tree level upper bound for the Higgs mass in the MSSM.

- Ways to get $M_{H_{SM}} \simeq 125$ GeV

  Due to the wide mass gap between M_Z and ~ 125 GeV it is necessary to consider mechanisms able to uplift the Higgs mass from its MSSM-like tree level value.

1. In the MSSM this may be achieved by sizable radiative corrections $\Delta_{\rm rad}$ which require large ($\gg 1$ TeV) values for at least one soft SUSY breaking stop mass term and/or A_t.
   But this leads to fine-tuning
   Such soft SUSY breaking terms generate, via loop effects, a soft SUSY breaking Higgs mass term $m^2_{H_u}$ (< 0) of the same order.
   On the other hand, combining the (tree level) minimization equations of the potential for the vevs v_u and v_d, one obtains

$$M_Z^2 = \frac{2(m^2_{H_d} - m^2_{H_u} \tan^2\beta)}{\tan^2\beta - 1} - 2\mu^2 \,. \tag{19}$$

   In the absence of fine tuning, there should be no large cancellations between the terms on the right hand side.
   Thus, large radiative corrections $\Delta_{\rm rad}$ generate a so-called "little fine tuning problem" in the MSSM.
   Moreover, the (effective) μ parameter should not be much larger than M_Z.
2. The second term in (18) is the well known NMSSM-specific contribution to the SM-like Higgs mass, which is numerically relevant for $\tan\beta \lesssim 6$ and large λ.
   Avoiding a Landau singularity below the GUT scale requires $\lambda \lesssim 0.75$, limiting the possible uplift of the mass of the SM-like Higgs state to $\lesssim 17$ GeV.

3. A third possibility to uplift the mass of the SM-like Higgs state uses level repulsion.
   - If the diagonal term $\mathcal{M}'^2_{S,33}$ in (15) associated with the mass of the singlet-like Higgs state S' is smaller than $\mathcal{M}'^2_{S,11}$, $H'_{SM} - S'$ mixing induced by the term $\mathcal{M}'^2_{S,13}$ in (15) shifts upwards the mass of the SM-like Higgs state H_{SM}.
   - The dominant contribution to $\mathcal{M}'^2_{S,13}$ originates from the first term $2\lambda v\mu$, which gets reduced by the second term $-\lambda v(A_\lambda + 2\nu)\sin 2\beta$. This reduction becomes small for moderate to large values of $\tan\beta$.
   - On the other hand, $H'_{SM} - S'$ mixing induces couplings of the lighter eigenstate H_S to electroweak gauge bosons, $b\bar{b}$ and gluons (through top quark loops). Such couplings of a state with a mass below 114 GeV are constrained by LEP.
   - This limits the region of λ for a sizable uplift the mass of the SM-like Higgs state to $\lambda \sim 0.04...0.1$, and thereby limits the possible uplift of the mass of the SM-like Higgs state to $\lesssim 8$ GeV.

The uplifts from #2 and #3 are NMSSM-specific and, in combination, are denoted by Δ_{NMSSM}.

- Considering further the mixing uplift possibility, #3, present constraints and future discoveries/constraints can originate from
  - direct searches for H_S in the diphoton final state, which had been carried out by ATLAS for $65\ \mathrm{GeV} < M_{H_S}$ and by CMS for $80\ \mathrm{GeV} < M_{H_S} < 115\ \mathrm{GeV}$.
  - measurements of the reduced signal rates/couplings (with respect to the SM) of H_{SM}. In the case of $H'_{SM} - S'$ mixing, these signal rates/couplings diminish proportional to the mixing angle.
  - possible production of H_S in decays of the MSSM-like states H/A.

- An aside on fine-tuning.
  - Since the fundamental parameters of the model are the masses and couplings at the GUT scale, one defines fine-tuning as

$$FT = Max\left\{\left|\frac{\partial \ln(M_Z)}{\partial \ln(p_i^{GUT})}\right|\right\} \tag{20}$$

    where p_i^{GUT} denote all dimensionful and dimensionless parameters (Yukawa couplings, mass terms and trilinear couplings) at the GUT scale. In the plots, only $FT < 1000$ points are shown.
  - Strong constraints on parameter spaces of SUSY extensions of the SM come from searches for gluinos $\tilde{g}$ and squarks $\tilde{q}$ of the first generation in events with jets and missing E_T.

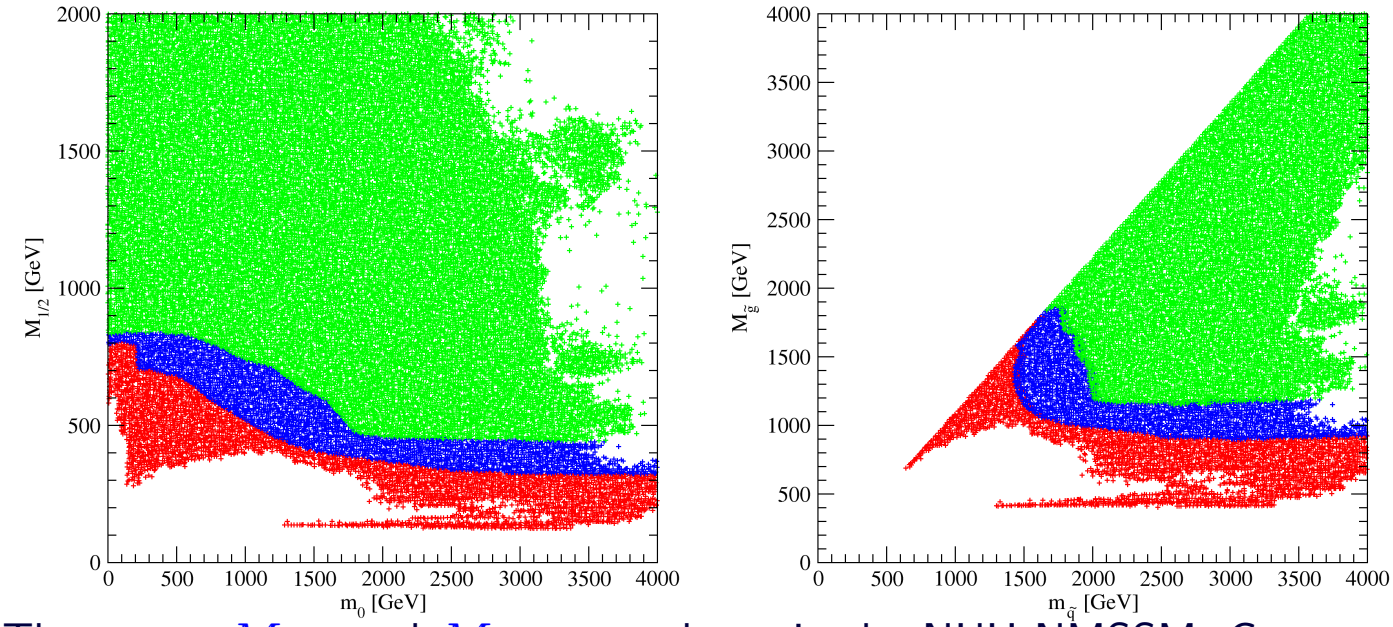

Figure 1: The $m_0 - M_{1/2}$ and $M_{\tilde{g}} - m_{\tilde{q}}$ planes in the NUH-NMSSM. Green: regions allowed by the 95% CL upper limits on signal events, blue: regions allowed in the presence of a singlino-like LSP, red: regions which are always excluded.

Exclusion limits in the $m_0 - M_{1/2}$ or $M_{\tilde{g}} - m_{\tilde{q}}$ planes in the NUH-NMSSM are very similar to the CMSSM if the LSP is bino-like, but can be alleviated in the presence of a light singlino-like LSP at the end of the cascades.

These lower bounds on the squark and gluino masses dominate the lower bounds on the fine-tuning FT defined in (20). In Fig. 2 we show FT as function of the squark and gluino masses, and the impact of the LHC constraints in the same color coding as in Fig. 1.

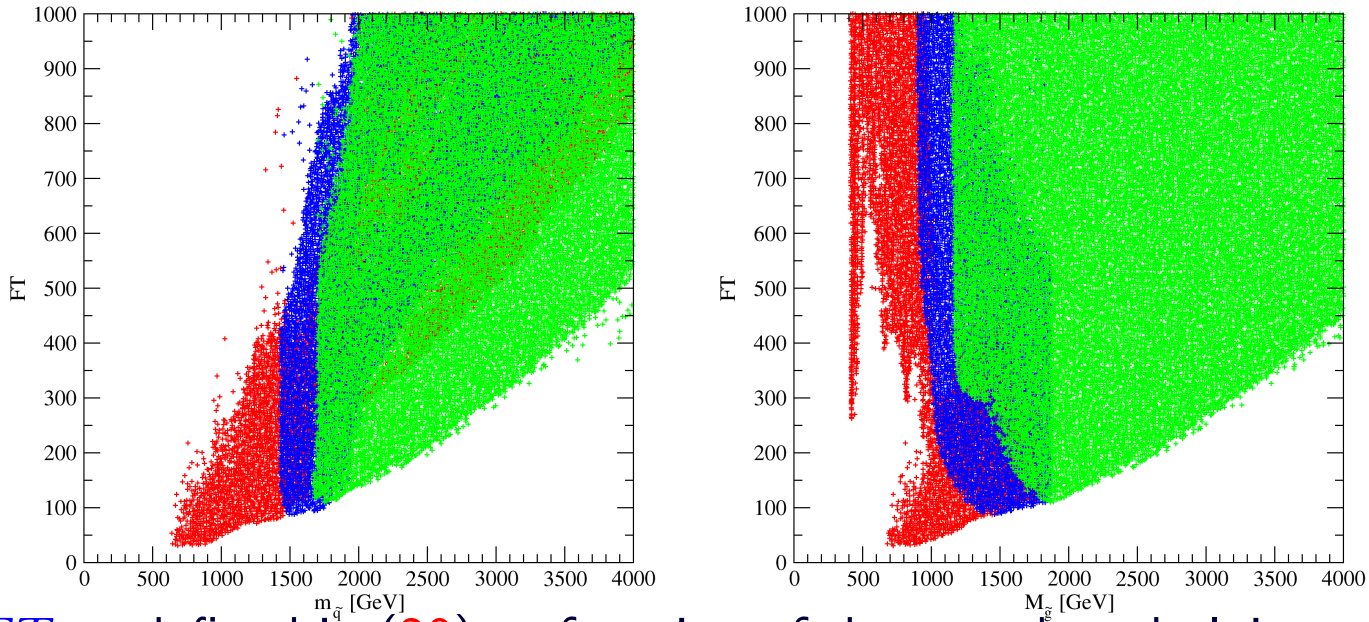

Figure 2: FT as defined in (20) as function of the squark and gluino masses, and the impact of the LHC constraints in the same color coding as in Fig. 1.

We see that the LHC forbidden red region increases the lower bound on FT from ~ 20 to $FT \gtrsim 80$; the NMSSM-specific alleviation (blue region) has a minor impact on FT.

The dominant contribution to FT in (20) originates typically from $M_{1/2}$ (i.e. the gluino mass at the GUT scale), or from the soft Higgs mass term $m^2_{H_u}$.

In the NMSSM, requiring unification of m_{H_u} and m_{H_d} with m_0, $\Rightarrow FT \gtrsim 400$.

In the MSSM, after imposing LHC constraints on squark and gluino masses, defining FT with respect to parameters at the GUT scale and allowing for non-universal Higgs mass terms at the GUT scale, one finds $FT \gtrsim 1000$.

– The small fine-tuning regions are further illustrated in Fig. 3.

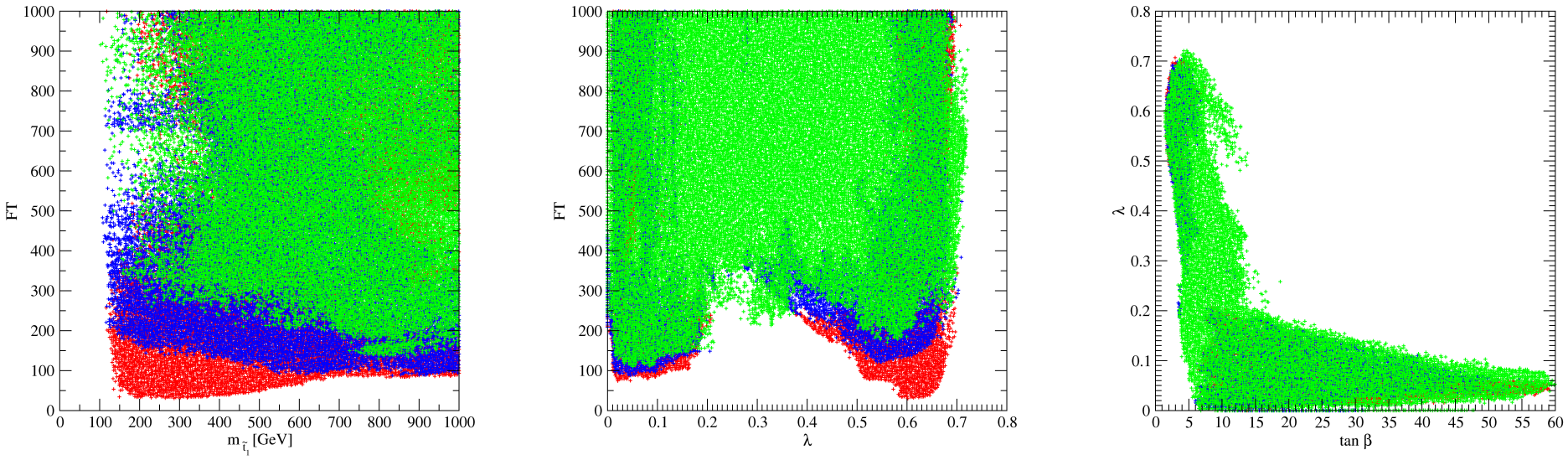

Figure 3: $H_2(SM)$ cases. Green=always ok; Blue=ok for mainly singlino LSP; Red=excluded after all constraints. Left: Fine tuning measure, FT, vs. λ. Right: λ vs. $\tan\beta$. The small λ region uses mixing uplift; the large λ region uses NMSSM specific extra terms.

Note that very low $m_{\tilde{t}_1} \sim 150$ GeV is possible (cancellations among $b \to s\gamma$ loops), but lowest FT is for $m_{\tilde{t}_1} \gtrsim 600$ GeV.

To assess further, requires scanning. To avoid too large fine tuning, Ellwanger et.al. use a more restricted scan.

$$700\ \mathrm{GeV} \leq M_{U_3} = M_{D_3} = M_{Q_3} \leq 1\ \mathrm{TeV}, \qquad -1\mathrm{TeV} \leq \mathrm{A_t} \leq 1\ \mathrm{TeV}\ . \quad (21)$$

Then $\Delta_{NMSSM} > 4\ \mathrm{GeV}$ is required.

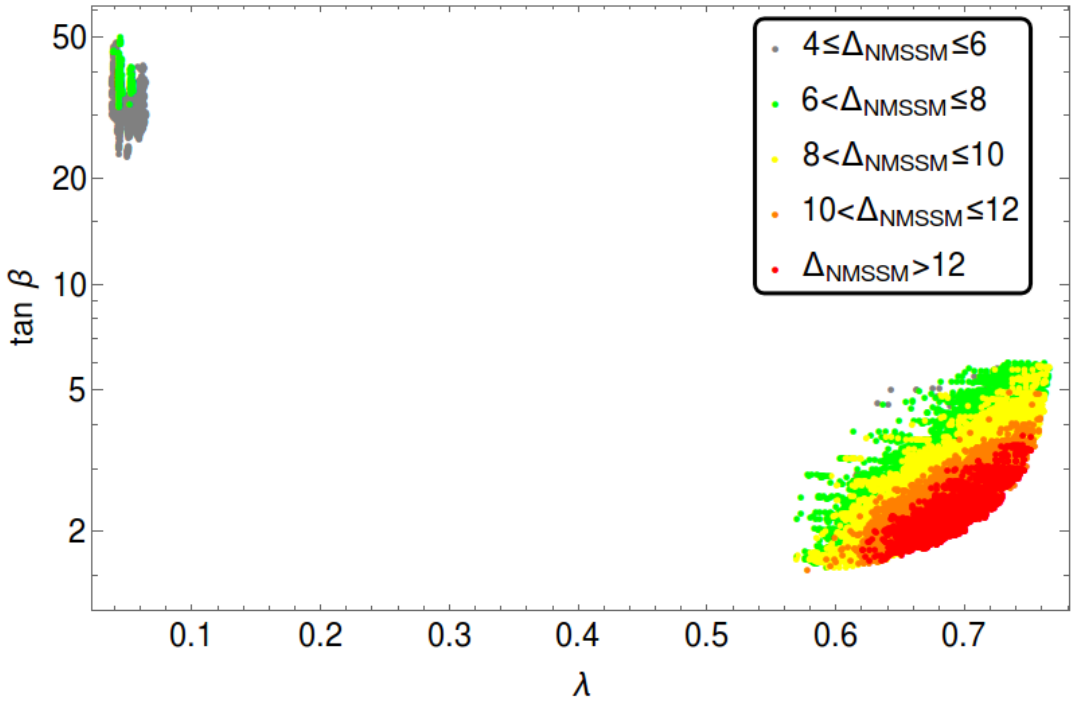

Figure 4: $\lambda - \tan\beta$ plane showing the viable points and Δ_{NMSSM} in the form of a color code. The island in the upper-left corner corresponds to the region where Δ_{NMSSM} originates from $H'_{SM} - S'$ mixing (LMIX), whereas the island in the large λ regime (LLAM) corresponds to the region with large contributions to Δ_{NMSSM} from the second term in (18).

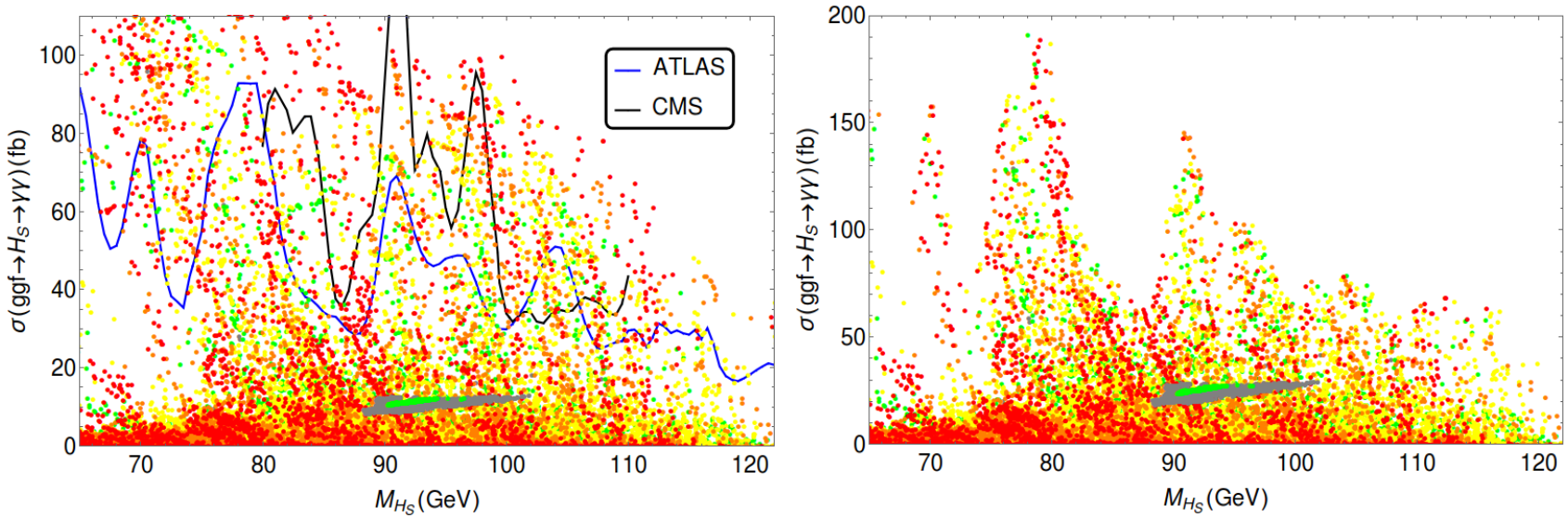

Figure 5: Left: Possible signal rates (in femtobarns) $\sigma(gg \to H_S \to \gamma\gamma)$ at a c.m. energy of $\sqrt{s} = 8$ TeV, together with the ATLAS and CMS limits from direct searches. The grey-green island corresponds to the LMIX region, the rest to the LLAM region. Right: Signal rates for the same process at $\sqrt{s} = 13$ TeV after applying the upper bounds from ATLAS and CMS.

- Possible signals associated with the H_S: $\gamma\gamma$ final state.

  We see in Figs. 5 that in the grey-green LMIX region M_{H_S} is confined to the mass range $88\ \mathrm{GeV} \lesssim \mathrm{M_{H_S}} \lesssim 102\ \mathrm{GeV}$, a consequence of the parameter range (21) and the corresponding lower limit on $\Delta_{\mathrm{NMSSM}} \gtrsim 4$ GeV. In order to obtain such values of Δ_{NMSSM} through $H'_{SM} - S'$ mixing, the mixing angle has to be relatively large leading to sizeable couplings of H_S to electroweak gauge bosons. These, in turn, are allowed by LEP only in the corresponding mass range where, actually, a mild excess of events is seen.

The recent ATLAS and CMS searches have not yet been sensitive to the possible signal rates $\sigma(gg \to H_S \to \gamma\gamma)$ in the LMIX region of the NMSSM. Fig. 5 (right) indicates, on the other hand, that the LMIX region could be completely tested once searches at $\sqrt{s} = 13$ TeV c.m. energy become sensitive to $\sigma(gg \to H_S \to \gamma\gamma) \sim 20$ fb.

Within the LLAM (large λ) region both M_{H_S} and $\sigma(gg \to H_S \to \gamma\gamma)$ can vary over much larger ranges and, indeed, the ATLAS and CMS searches have started to test parts of the LLAM region where this signal rate is particularly large. On the other hand this signal rate can also be quite small in the LLAM region where $H'_{SM} - S'$ mixing is possible, but not mandatory. This part of the LLAM region will be hard to test via searches for direct H_S production.

Above, points with $M_{H_S} < 60$ GeV were not shown. They are present only in the LLAM region, but are very few in number. This is because $H_{SM} \to H_S H_S$ decays would reduce the observed H_{SM} signal rates into SM-like final states to inadmissible levels for most parameter choices. However, the $H_{SM} - H_S - H_S$ coupling can be small for large λ, due to (rare) accidental cancellations among the various contributing terms.

- What about the H_{SM}?

All current constraints were incorporated above. But, deviations may be detected in the future. Correlations among deviations will clearly separate the LLAM from the LMIX type scenarios. Only in the LLAM case can the H_{SM} be extremely SM-like.

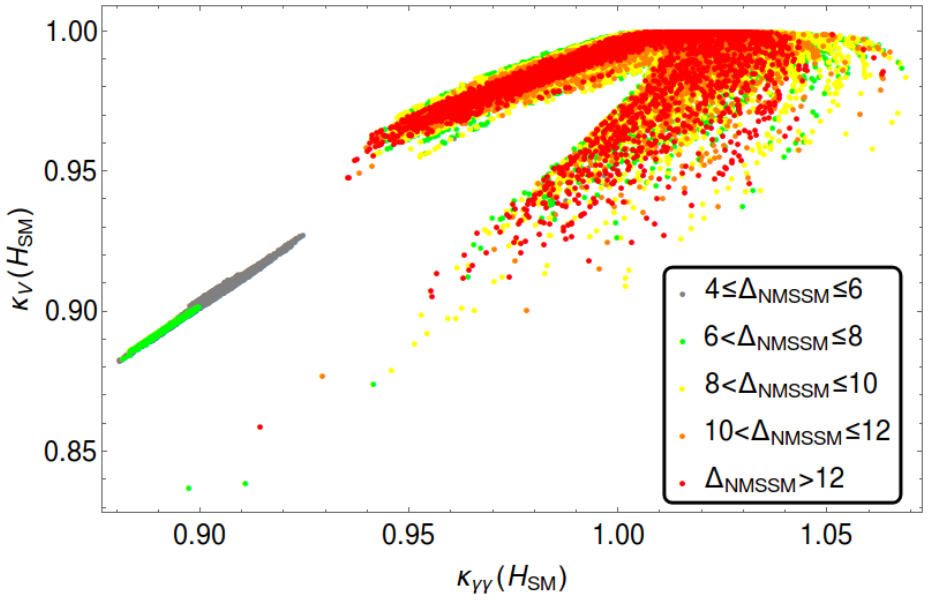

Figure 6: Reduced couplings $\kappa_V(H_{SM})$ and $\kappa_{\gamma\gamma}(H_{SM})$ for the viable points, including a color code for $\Delta_{\rm NMSSM}$.

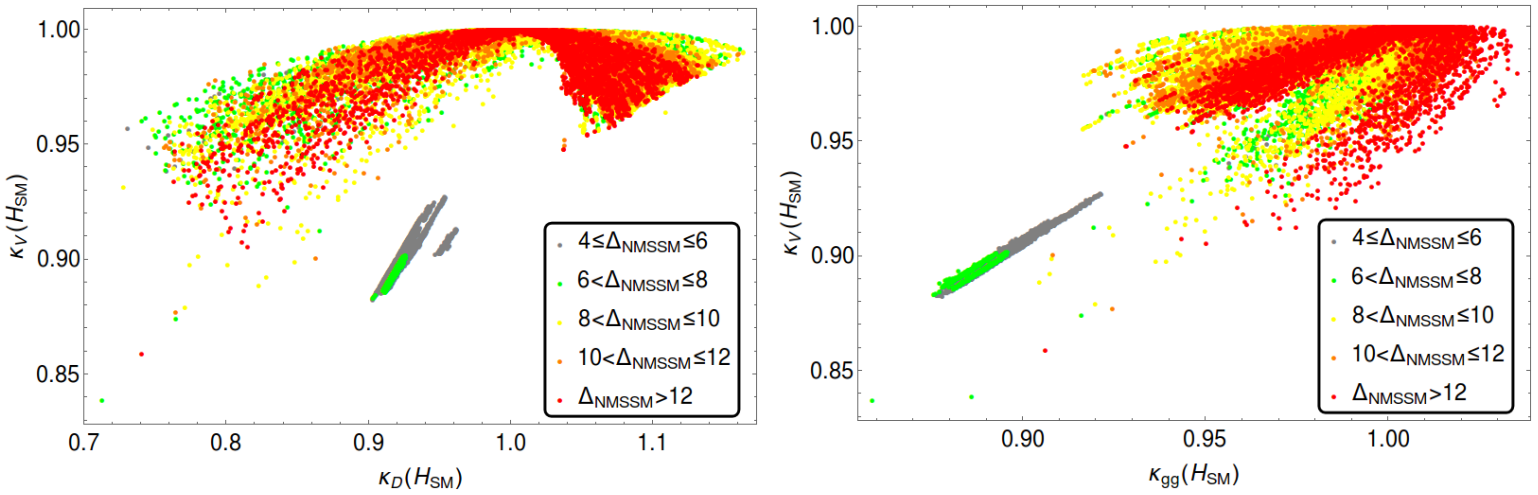

Figure 7: Correlations of $\kappa_V(H_{SM})$ with the reduced couplings of H_{SM} to down-type fermions (left) and gluons (right). In both plots the LLAM and LMIX regions are clearly separated.

- Correlations between reduced couplings for the H_{SM} and $\sigma(gg \to H_S \to \gamma\gamma)$ might be informative.

  The LLAM region can become visible either by an enhanced $\sigma(gg \to H_S \to \gamma\gamma)$ or a reduced $\kappa_V(H_{SM})$, but not both. Unfortunately, a low signal rate $\sigma(gg \to H_S \to \gamma\gamma)$ as well as $\kappa_V(H_{SM}) \sim 1$ are possible simultaneously. From the right hand side of Figs. 8 we see that enhanced signal rates $\sigma(gg \to H_S \to \gamma\gamma) \gtrsim 50$ fb and enhanced reduced couplings $\kappa_{\gamma\gamma}(H_{SM})$ are incompatible in the LLAM region.

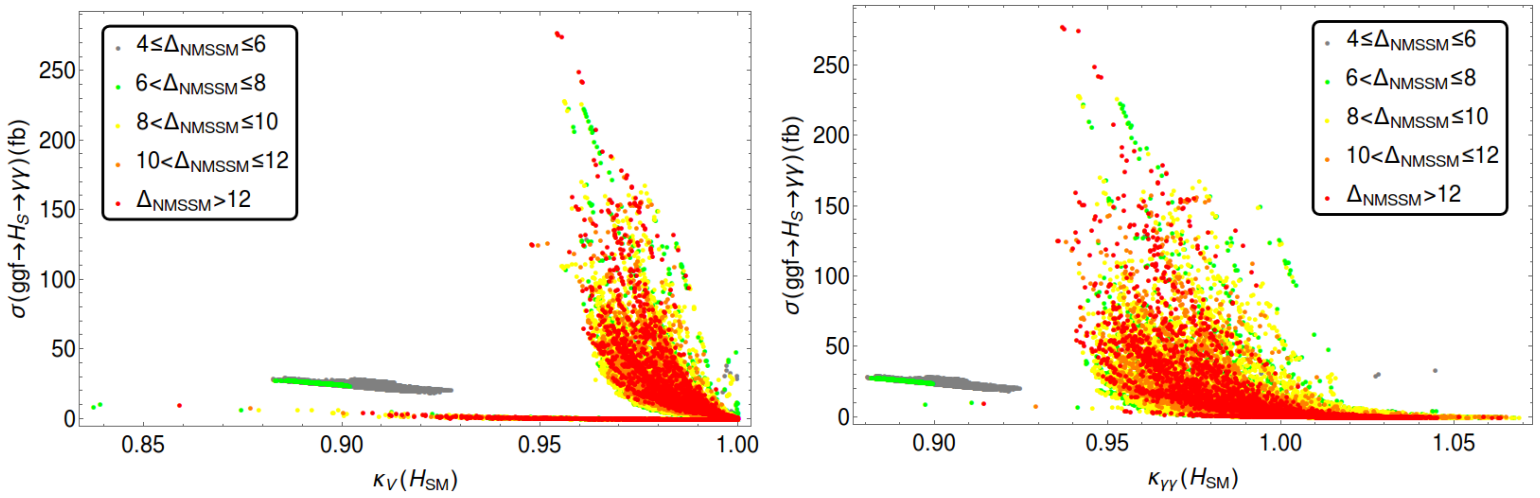

Figure 8: Left: Correlations among the diphoton signal rate of H_S and $\kappa_V(H_{SM})$. Right: Correlations among the diphoton signal rate of H_S and $\kappa_{\gamma\gamma}(H_{SM})$.

- H_S production via decays of heavy states H/A

  First, the masses of H/A possible in the LMIX/LLAM regions of the NMSSM are shown in Fig. 9 in the $\tan\beta - M_A$ plane — plotted points those not ruled out by searches for MSSM-like H/A in the $\tau^+\tau^-$ final state (from here onwards, M_A denotes the physical mass of the MSSM-like CP-odd state A):

  – The LMIX region with large $\tan\beta$ features very heavy H/A states, to which searches at the run I have not been sensitive (and which will be hard to search for at the run II).

– The LLAM region is characterized by lower $\tan\beta$ such that the associated production of H/A states with b quarks is not very enhanced; instead, their production via gluon fusion becomes feasible in principle.
– The part of the LLAM region where $M_A \gtrsim 500$ GeV and $\tan\beta \gtrsim 3$ corresponds, however, to the difficult region where the reduced couplings of H_{SM} are very SM-like and H_S has a low signal rate in the $\gamma\gamma$ channel; in this region also the search for the MSSM-like states H/A seems difficult.

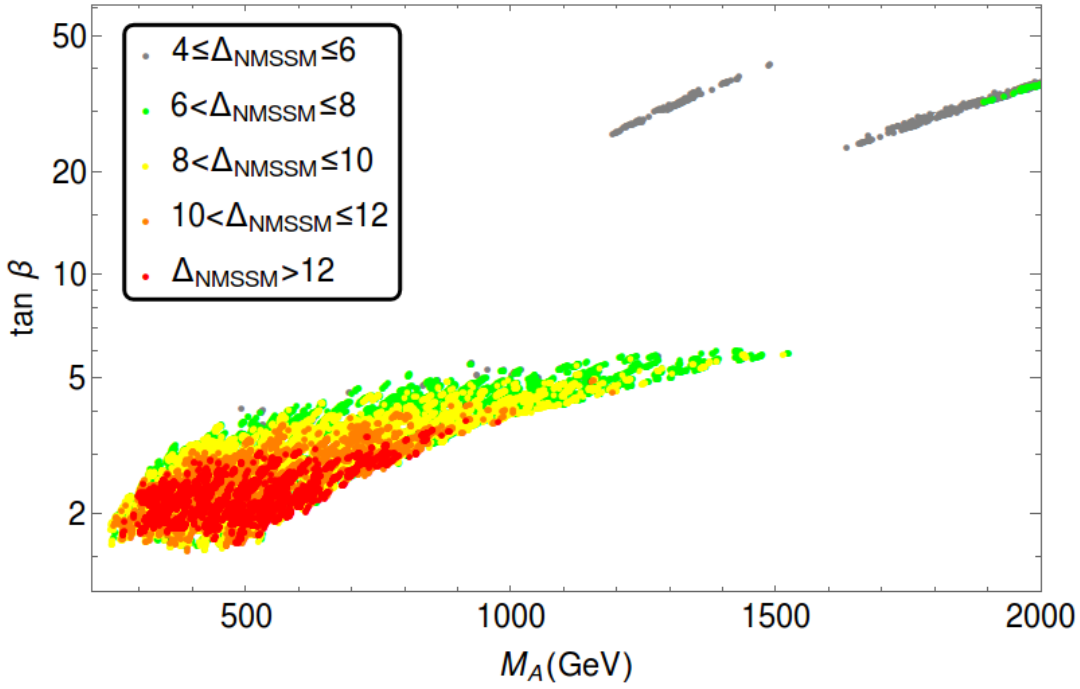

Figure 9: Viable points in the $\tan\beta - M_A$ plane.

- Promising decays of H/A into H_S are $A \to Z + H_S$ and $H \to H_{SM} + H_S$.

  Since the kinematics of $A \to Z + H_S$ is very similar to the one of $H \to Z + A_S$ investigated in Bomark et.al. (summarized shortly), we employ these studies of the $Z \to l^+l^-$ ($l \equiv e, \mu$) and $A_S \to b\bar{b}$ final states, including their sensitivity curves as function of M_{A_S} (now interpreted as M_{H_S}).

- The signal cross section $\sigma(ggF \to A \to Z + H_S)$ is shown on the left hand side of Fig. 10 as function of M_A; clearly, visible signal rates can only be expected for $M_A \lesssim 400$ GeV within the LLAM region.

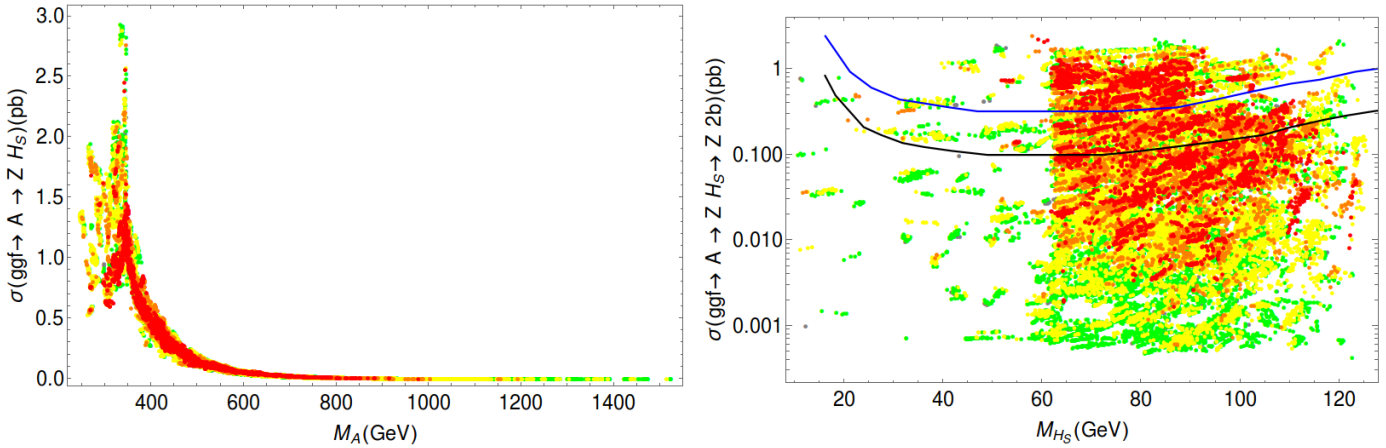

Figure 10: Left: Signal cross section $\sigma(ggF \to A \to Z + H_S)$ as function of M_A for a c.m. energy of $\sqrt{s} = 13$ TeV. Right: Signal cross section $\sigma(ggF \to A \to Z + b + \bar{b})$ as function of M_{H_S}, compared to the expected sensitivities for a integrated luminosities of 300 fb^{-1} (blue) and 3000 fb^{-1} (black).

On the right hand side of Fig. 10 the range of signal cross sections $\sigma(ggF \to A \to Z + b + \bar{b})$ is shown as function of M_{H_S}, and compared to the expected sensitivities at the run II of the LHC for integrated luminosities of $300\ \mathrm{fb}^{-1}$ (blue) and $3000\ \mathrm{fb}^{-1}$ (black). Hence, detectable signal rates in this channel are indeed possible in the LLAM region of the NMSSM without, however, covering it completely.

- In Fig. 11 we show the cross section $\sigma(ggF \to H \to H_{SM} + H_S)$ as function of M_H for a c.m. energy of $\sqrt{s} = 13$ TeV on the left, and the (dominant) signal cross section $\sigma(ggF \to H \to H_{SM} + H_S \to 4b)$ as function of M_{H_S} on the right.

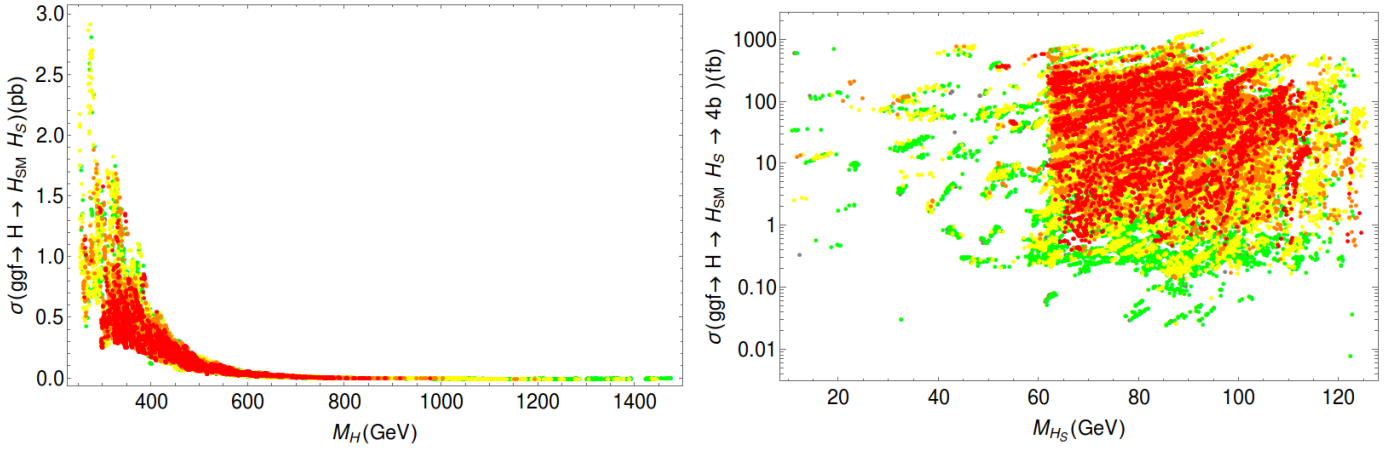

Figure 11: Total ggF production cross section for $H \to H_{SM} + H_S$ at $\sqrt{s} = 13$ TeV (left), and for the $b\bar{b}b\bar{b}$ final state versus the mass of H_S (right).

Of course, one is handicapped by the a priori unknown mass of H_S.

- Search strategies including background studies can possibly be pursued along the lines proposed by Bomark et.al. for searches for a light NMSSM pseudoscalar A_S.

  In the region of the NMSSM parameter space considered here A_S is, however, not particularly light; in the (wider) LLAM region, M_{A_S} varies from ~ 80 to ~ 300 GeV, but from ~ 60 to ~ 180 GeV in the (narrower) LMIX region.

- The light pseudoscalar possibility

  Two notations employed in the recent papers: A_S and A_1.

  In the $\mathbb{Z}_3$-invariant NMSSM, after eliminating the Goldstone mode, $\mathcal{M}_P^2$ simplifies to

$$\begin{aligned} \mathcal{M}^2_{P,11} &= \frac{2\,\lambda s(A_\lambda + \kappa s)}{\sin 2\beta}\,, \\ \mathcal{M}^2_{P,22} &= \lambda(A_\lambda + 4\kappa s)\frac{v^2 \sin 2\beta}{2s} - 3\kappa A_\kappa\, s\,, \\ \mathcal{M}^2_{P,12} &= \lambda(A_\lambda - 2\kappa s)\, v \end{aligned} \tag{22}$$

  The matrix element $\mathcal{M}^2_{P,11}$ corresponds to the mass squared M_A^2 of the (only physical) CP-odd scalar A of the MSSM.

As is well known, there is an R symmetry limit of $A_\lambda, A_\kappa \to 0$ in which the lightest CP-odd state has $M_{A_1} = 0$. In practice, $A_\lambda = 0$ is not possible because of CP-even sector constraints. But, one can still achieve $M_{A_1} \sim 0$.

- The A_1 in the $H_2 = H_{SM}$ scenario preferred by lower fine-tuning.

  Both Ellwanger et.al. (1512.04281) and Bomark et.al (1403.8393) have examined the relevant phenomenology. The latter paper explicitly restricts considerations to LLAM type scenarios with $M_{A_1} \leq 150$ GeV.

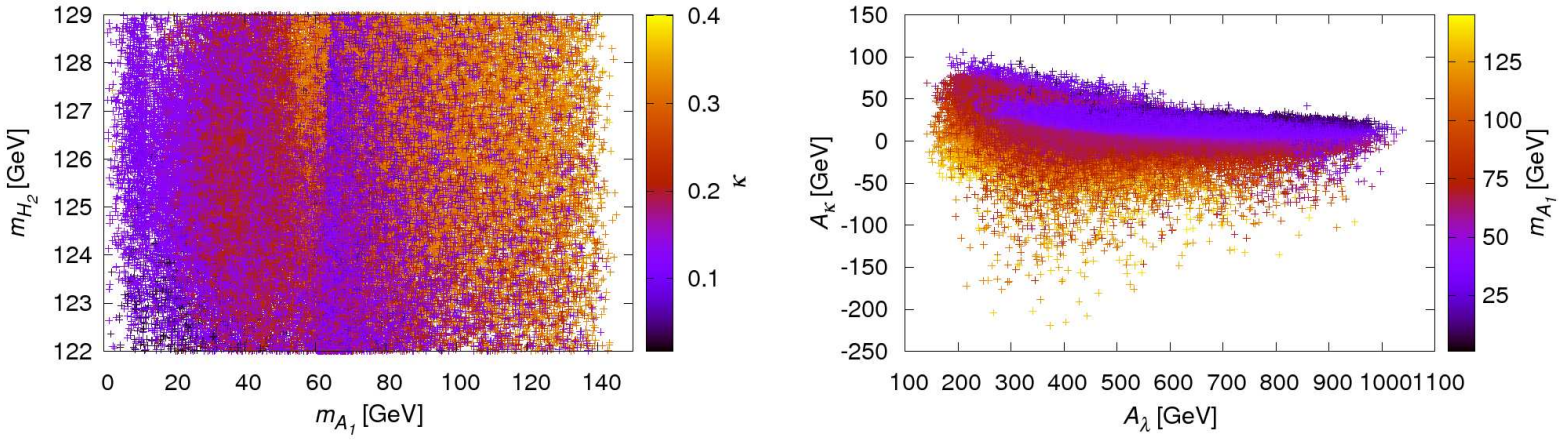

Figure 12: Case with $H_{\rm SM} = H_2$: (a) mass of H_2 vs. that of A_1, with the heat map showing the distribution of κ; (b) the parameter A_λ vs. the parameter A_κ, with the heat map showing the distribution of the mass of A_1. From 1403.8393.

How do we observe a light A_1?

1. $b\bar{b}A_1$ has too low a cross section for the modest $\tan\beta$ values of the LLAM scenarios. May be useful for LMIX scenarios.
2. $H_{SM} = H_2 \to A_1 A_1$ can still be substantial despite existing limits on unseen decays of the SM-like Higgs. But, $H_2 \to Z A_1$ has small cross sections.

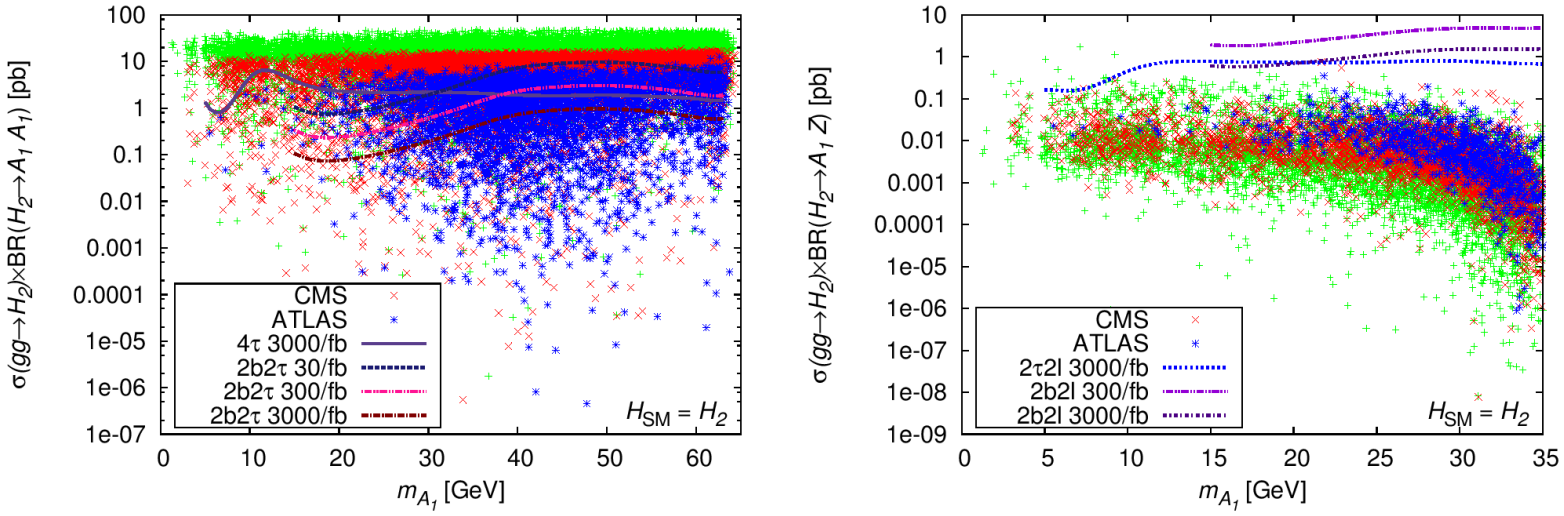

Figure 13: Total cross sections in the case with $H_{\rm SM} = H_2$ for (a) the $gg \to H_{\rm SM} \to A_1 A_1$ process and (b) the $gg \to H_{\rm SM} \to A_1 Z$ process. The red and the blue points satisfy the CMS and the ATLAS constraints on $H_2 = H_{SM}$. In green are the unfiltered points satisfying neither of these constraints. Also shown are the sensitivity curves for various final state combinations. From 1403.8393.

3. The $H_S = H_1 \to A_1 A_1$ is likely to be the most sensitive channel. One sees in figure 14(a) that almost all the points complying with the current CMS and/or ATLAS constraints on the $H_{SM} = H_2$ are potentially discoverable, even at $\mathcal{L} = 30/\text{fb}$.
   Finally, In figure 14(b), we see that the prospects for the discovery of A_1 via the $H_1 \to A_1 Z$ channel are non-existent in this case too.

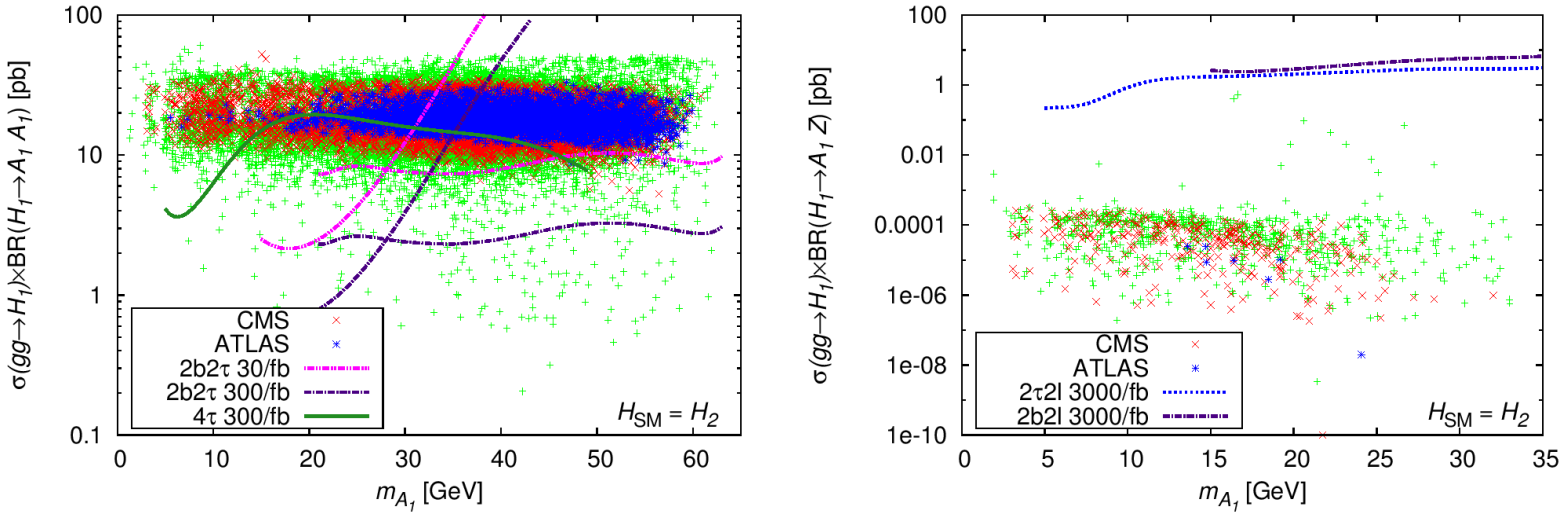

Figure 14: Total cross sections in the case with $H_{\rm SM} = H_2$ for (a) the $gg \to H_1 \to A_1 A_1$ process and (b) the $gg \to H_1 \to A_1 Z$ process. The color convention for the points is the same as in figure 13. From 1403.8393.

Theses results are somewhat similar to those of 1512.04281 (Ellwanger et.al.) except that the latter does not have any clear lower bound on the allowed $H_1 \to A_1 A_1$ cross sections.

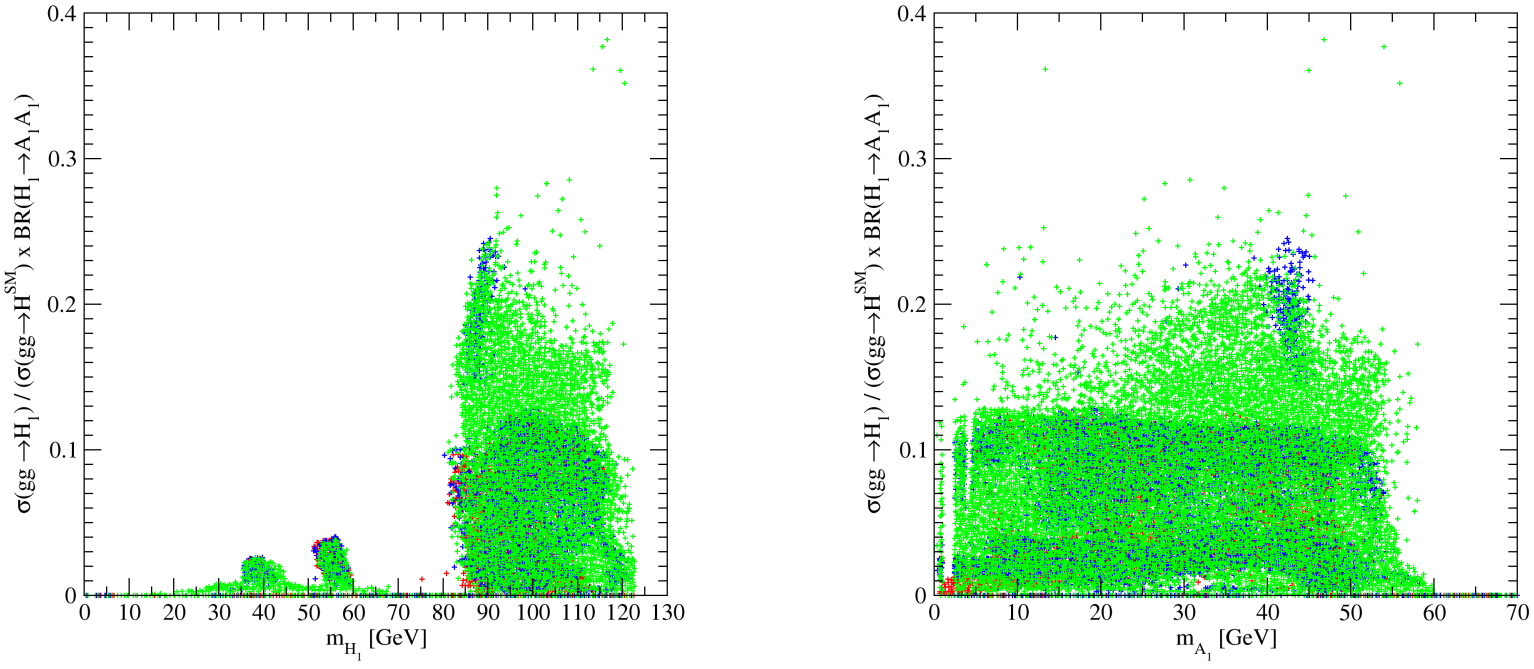

Figure 15: Total ggF production cross section for $H_S = H_1 \to A_1 A_1$ relative to ggF cross section for $H_{SM} = H_2$ at $\sqrt{s} = 13$ TeV as a function of M_{H_1} (left) and M_{A_1} (right). Note that very small M_{A_1} values are possible. In this color scheme, blue points have better FT because of more difficult SUSY singlino LSP scenarios and red are simply excluded. From 1512.04281.

750 GeV diphoton signal

There are two NMSSM realizations:

1. Interpreting 750 GeV Diphoton Excess in Plain NMSSM (Marcin Badziak, Marek Olechowski, Stefan Pokorski, Kazuki Sakurai) arXiv:1603.02203.

2. A 750 GeV Diphoton Signal from a Very Light Pseudoscalar in the NMSSM (Ulrich Ellwanger and Cyril Hugonie) arXiv:1602.03344.

- In #1, there is a very singlet A_1 which decays to 2 photons and which is produced via the cascade decay $A_2 \to S A_1$ where S is a singlet CP-even Higgs. A_2 has a large production cross section since it is mainly MSSM-like.

- In #2, there several possibilities are discussed. To my thinking, the most attractive is one where H_1 is SM-like, H_2 has enhanced $b\bar{b}$ coupling and so strong production in $b\bar{b}H_2$.

  H_2 then decays to $A_1 A_1$ and has a total width of ~ 7 GeV (i.e. this is not a narrow width case and thus matches ATLAS better than some 750 models).

A_λ and A_κ are adjusted so that M_{A_1} is just slightly above $2m_\mu$ (obviously a fine tuning), and then the A_1 will have signifiant branching ratio to $\gamma\gamma$ and a path length such that many A_1A_1 events will be accepted as $\gamma\gamma$ events.

Since it is H_1 that is SM-like, this scenario suffers from a rather small M_{H_1}.

Some features of this and other scenarios are tabulated below. The other BP's get a large enough signal rate by having both H_2 and H_3 near 750 GeV.

Couplings and mass parameters	BP1	BP2	BP3	BP4
λ	0.528	0.212	0.0332	0.0644
κ	1.65	0.75	0.121	0.215
$\tan\beta$	9.57	16.8	15.5	14.5
μ (GeV)	138.5	101.1	102.3	111.3
A_λ (GeV)	32.2	15.6	0.0	0.0
A_κ (GeV)	1.16	7.67×10^{-2}	-4.69×10^{-4}	-1.49×10^{-3}
$M_{\rm squarks}$ (TeV)	6	7.5	2	3
A_t (TeV)	-3.48	-3.95	3	3

Table 1: Parameters for the four benchmark points. The soft Susy breaking gaugino masses are $M_1 = 600$ GeV (500 GeV for BP1), $M_2 = 1$ TeV, $M_3 = 3$ TeV, all squarks are assumed degenerate, and all slepton masses are 300 GeV (with vanishing trilinear couplings).

	BP1	BP2	BP3	BP4
M_{H_1} (GeV)	122.1	124.3	123.7	122.2
M_{H_2} (GeV)	750	730	744	740
M_{H_3} (GeV)	1003	762	750	750
M_{A_1} (MeV)	211.3	211.1	548.7	510.3
M_{A_2} (GeV)	763	747	748	745
$M_{H^\pm}$ (GeV)	757	749	752	749
$\sigma_{ggF}(H_2)$ (fb)	4.8	2.2	1.7	1.9
$\sigma_{bbH}(H_2)$ (fb)	36.8	67.2	44.7	44.9
$\sigma_{ggF}(H_3)$ (fb)	0.1	1.8	2.0	1.9
$\sigma_{bbH}(H_3)$ (fb)	0.2	52.5	54.3	44.3
$BR(H_2 \to A_1 A_1)$	0.51	0.66	0.082	0.21
$BR(H_3 \to A_1 A_1)$	0.72	0.53	0.048	0.16
$BR(A_1 \to \gamma\gamma)$	0.74	0.73	0.72	0.66
$\Gamma_{tot}(A_1)$ (10^{-13} GeV)	1.74	0.65	7500	19000
$l(A_1)$ at 375 GeV	2 m	5.5 m	0.18 mm	0.08 mm
Signal cross section (fb)	4.6	3.7	3.4	6.7

Table 2: Higgs masses, production cross sections and branching fractions for the 4 benchmark points. For the points BP1 and BP2, the signal cross section takes into account losses from A_1 decays beyond 2 m according to a factor $\left(1 - e^{-2/l}\right)^2$ with l in m. For the points BP3 and BP4 the $BR(A_1 \to \gamma\gamma)$ includes the $BR(A_1 \to 3\pi^0)$.

Conclusions

- The Higgs responsible for EWSB has emerged and is really very SM-like.
- The CNMSSM-NUHM (universal GUT-scale with NUHM relaxation boundary conditiona) is still quite an attractive model with lower fine-tuning than the MSSM. Indeed, the CNMSSM-NUHM fine-tuning of $FT \sim 100$ is comparable to that of neutral-naturalness models which go to the GUT scale.
- The NMSSM leads to a plethora of possible signals, especially in the Higgs sector.
- But, there could be increased difficulty for detecting squarks and gluinos due to cascades involving singlinos.